Inorg. Chem. **2003**, *42*, 6616–6628

Excited-State Energy-Transfer Dynamics of Self-Assembled Imine-Linked Porphyrin Dyads

Igor V. Sazanovich,[†] Arumugham Balakumar,[‡] Kannan Muthukumaran,[‡] Eve Hindin,[†] Christine Kirmaier,[†] James R. Diers,[§] Jonathan S. Lindsey,*[,‡] David F. Bocian,*[,§] and Dewey Holten*[,†]

Departments of Chemistry, Washington University, St. Louis, Missouri 63130-4899, North Carolina State University, Raleigh, North Carolina 27695-8204, and University of California, Riverside, California 92521-0403

Received May 23, 2003

Toward the development of new strategies for the synthesis of multiporphyrin arrays, we have prepared and characterized (electrochemistry and static/time-resolved optical spectroscopy) a series of dyads composed of a zinc porphyrin and a free base porphyrin joined via imine-based linkers. One dyad contains two zinc porphyrins. Imine formation occurs under gentle conditions without alteration of the porphyrin metalation state. Five imine linkers were investigated by combination of formyl, benzaldehyde, and salicylaldehyde groups with aniline and benzoic hydrazide groups. The imine-linked dyads are quite stable to routine handling. The excited-state energy-transfer rate from zinc to free base porphyrin ranges from $(70\ \text{ps})^{-1}$ to $(13\ \text{ps})^{-1}$ in toluene at room temperature depending on the linker employed. The energy-transfer yield is generally very high (>97%), with low yields of deleterious hole/electron transfer. Collectively, this work provides the foundation for the design of multiporphyrin arrays that self-assemble via stable imine linkages, have predictable electronic properties, and have comparable or even enhanced energy-transfer characteristics relative to those of other types of covalently linked systems.

Introduction

The organization of multiple porphyrins into arrays provides the basis for both natural and synthetic materials with diverse functions.[1−18] Two distinct methods generally have been employed for creating synthetic multiporphyrin arrays: (1) stepwise syntheses of covalently linked systems and (2) self-assembly of noncovalently linked systems in which the components are held together via weak interactions such as hydrogen-bonding, electrostatic interactions, hydrophobic forces, and/or apical metal coordination. Each approach has strengths and weaknesses. The stepwise synthesis

* To whom correspondence should be addressed. E-mail: holten@wuchem.wustl.edu (D.H.); jlindsey@ncsu.edu (J.S.L.); David.Bocian@ucr.edu (D.F.B.).
[†] Washington University.
[‡] North Carolina State University.
[§] University of California.

(1) Harvey, P. D. In *The Porphyrin Handbook*; Kadish, K. M., Smith, K. M., Guilard, R., Eds.; Academic Press: San Diego, CA, 2003; Vol. 18, pp 63−250.
(2) Wöhrle, D.; Schnurpfeil, G. In *The Porphyrin Handbook*; Kadish, K. M., Smith, K. M., Guilard, R., Eds.; Academic Press: San Diego, CA, 2003; Vol. 17, pp 177−246.
(3) Collman, J. P.; Boulatov, R.; Sunderland, C. J. In *The Porphyrin Handbook*; Kadish, K. M., Smith, K. M., Guilard, R., Eds.; Academic Press: San Diego, CA, 2003; Vol. 11, pp 1−49.
(4) Alessio, E.; Iengo, E.; Marzilli, L. G. *Supramol. Chem.* **2002**, *14*, 103−120.
(5) Holten, D.; Bocian, D. F.; Lindsey, J. S. *Acc. Chem. Res.* **2002**, *35*, 57−69.
(6) Burrell, A. K.; Officer, D. L.; Plieger, P. G.; Reid, D. C. W. *Chem. Rev.* **2001**, *101*, 2751−2796.
(7) Aratani, N.; Osuka, A. *Macromol. Rapid Commun.* **2001**, *22*, 725−740.
(8) Balzani, V.; Ceroni, P.; Juris, A.; Venturi, M.; Campagna, S.; Puntoriero, F.; Serroni, S. *Coord. Chem. Rev.* **2001**, *219*−*221*, 545−572.
(9) Sanders, J. K. M. In *The Porphyrin Handbook*; Kadish, K. M., Smith, K. M., Guilard, R., Eds.; Academic Press: San Diego, CA, 2000; Vol. 3, pp 347−368.
(10) Swiegers, G. F.; Malefetse, T. J. *Chem. Rev.* **2000**, *100*, 3483−3537.
(11) Imamura, T.; Fukushima, K. *Coord. Chem. Rev.* **2000**, *198*, 133−156.
(12) Wojaczyski, J.; Latos-Grazynski, L. *Coord. Chem. Rev.* **2000**, *204*, 113−171.
(13) Flamigni, L.; Barigelletti, F.; Armaroli, N.; Collin, J.-P.; Dixon, I. M.; Sauvage, J.-P.; Williams, J. A. G. *Coord. Chem. Rev.* **1999**, *190*−*192*, 671−682.
(14) Tamiaki, H. *Coord. Chem. Rev.* **1996**, *148*, 183−197.
(15) Kurreck, H.; Huber, M. *Angew. Chem., Int. Ed. Engl.* **1995**, *34*, 849−866.
(16) Gribkova, S. E.; Evstigneeva, R. P.; Luzgina, V. N. *Russ. Chem. Rev.* **1993**, *62*, 963−979.
(17) (a) Gust, D.; Moore, T. A.; Moore, A. L. *Acc. Chem. Res.* **1993**, *26*, 198−205. (b) Gust, D.; Moore, T. A. *Topics Curr. Chem.* **1991**, *159*, 103−151.
(18) Wasielewski, M. R. *Chem. Rev.* **1992**, *92*, 435−461.

10.1021/ic034558u CCC: $25.00
Published on Web 09/17/2003

of covalently linked arrays enables each component to be anchored irreversibly in a specific location in a 3-dimensional architecture. However, the construction of such arrays is often laborious. On the other hand, the self-assembly approach only requires synthesis of component parts and relies on the specificity of noncovalent interactions to produce the desired array. Disadvantages of the self-assembly approach are that (1) the strength of the interactions between components is often insufficient to give a high yield of the target array at equilibrium and (2) multiple products of similar composition may be formed. For photochemical studies, it is essential to prepare a distinct target of known composition and architecture. The requirement of distinct molecular integrity can limit the application of self-assembled systems because the typical use of dilute solutions ($\sim\mu$M) can result in disassembly of the self-assembled array.

The inspiration for reliance on self-assembly in chemical synthesis has often emanated from biology where self-assembly affords elaborate molecular assemblies.[19,20] The development of chemical self-assembly processes that are comparable to those in biological systems is a great challenge. The molecular interactions in biological self-assembly processes typically encompass noncovalent interactions as well as covalent bond-forming reactions (giving disulfides, imines, etc.). Self-assembly processes built around reversible covalent bond formation facilitate construction of elaborate architectures while also affording more stable assemblies than those typically obtained via noncovalent interactions. Covalent self-assembly[19] also forms the basis for studies in dynamic combinatorial chemistry.[21] Numerous multiporphyrin arrays have been prepared by metal-coordination-mediated self-assembly[4,8−13] whereas only a few have been prepared containing imine linkages.[22] The metal-coordination assembly processes encompass interactions that range from relatively weak (e.g., coordination of nitrogenous bases at the porphyrin apical metal site) to quite strong (e.g., chelation of multivalent metals by multidentate ligands attached to the perimeter of the porphyrin) and thus can exhibit behavior spanning that typical of noncovalent interactions and covalent bonds.

In covalently linked multiporphyrin arrays that exhibit light-harvesting properties, the linker serves both a mechanical function and an electronic function. The mechanical function is to hold the porphyrins in a fixed architecture. The electronic function is to provide a conduit for communication among the porphyrins, thereby enhancing the rate and yield of excited-state energy transfer. The rate of such through-bond (TB) energy transfer can be much faster than through-space (TS) energy transfer. Indeed, in dyads composed of a zinc porphyrin and a free base porphyrin joined by a 4,4′-diphenylethyne linker, the observed $(24\ \text{ps})^{-1}$ rate of transfer originates from a TB energy-transfer rate of $(25\ \text{ps})^{-1}$ and a TS energy-transfer rate of $(720\ \text{ps})^{-1}$.[5] Thus, the electronic communication provided by the linker is the dominant contributor to the observed energy-transfer process.

Chart 1

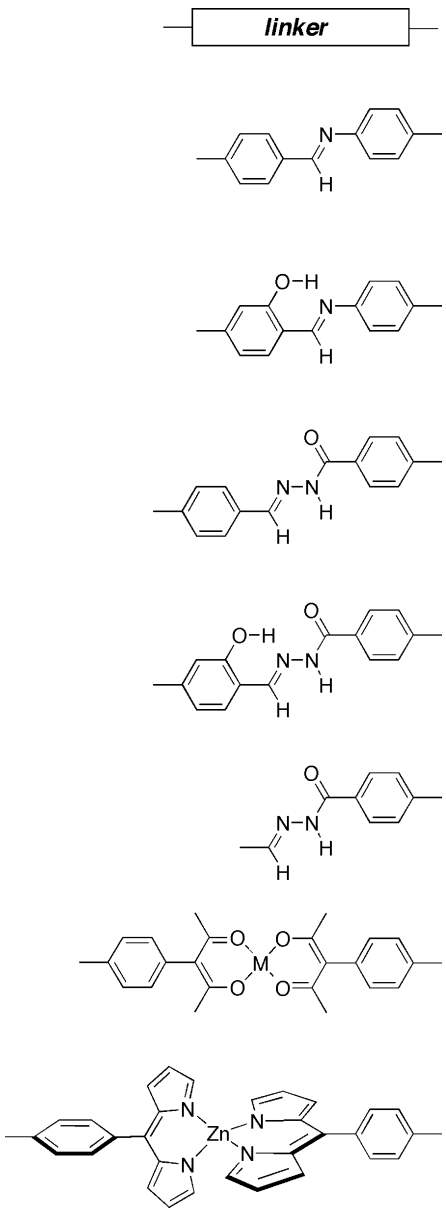

For the covalent self-assembly of multiporphyrin light-harvesting arrays, the ideal linker should have the following properties: (1) afford the self-assembled product in high yield; (2) form under neutral conditions without demetalation of the porphyrins; (3) provide directional assembly enabling rational formation of dyads composed of metalloporphyrins in distinct metalation states; (4) provide efficient TB electronic communication between the porphyrins; (5) not participate in any deleterious excited-state quenching processes; and (6) be stable toward oxidation and reduction. A number of candidates for such linkers are shown in Chart 1. Five linkers are built around imine motifs; one is a metal−acac complex, and one is a bis(dipyrrinato)metal(II) complex.

In this paper, we describe the synthesis of porphyrin building blocks bearing functional groups for formation of

(19) Lindsey, J. S. *New J. Chem.* **1991**, *15*, 153−180.
(20) Lawrence, D. S.; Jiang, T.; Levett, M. *Chem. Rev.* **1995**, *95*, 2229−2260.
(21) Rowan, S. J.; Cantrill, S. J.; Cousins, G. R. L.; Sanders, J. K. M.; Stoddart, J. F. *Angew. Chem., Int. Ed.* **2002**, *41*, 898−952.
(22) Screen, T. E. O.; Blake, I. M.; Rees, L. H.; Clegg, W.; Borwick, S. J.; Anderson, H. L. *J. Chem. Soc., Perkin Trans. 1* **2002**, 320−329.

Chart 2

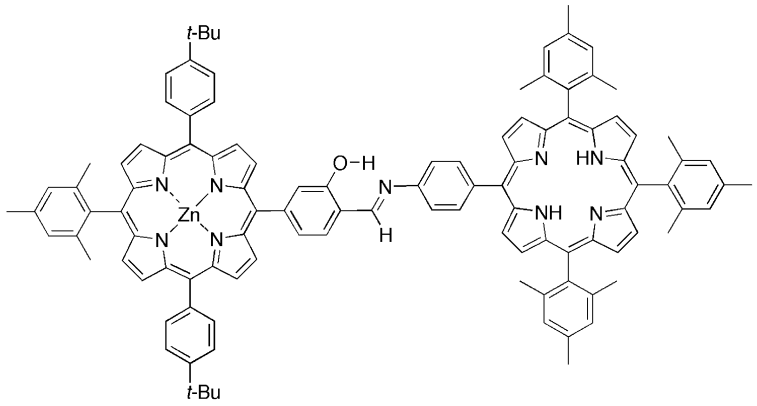

Dyad-1

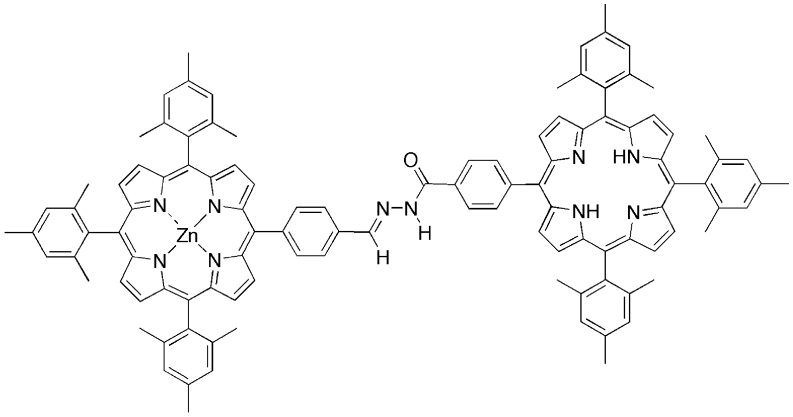

Dyad-2

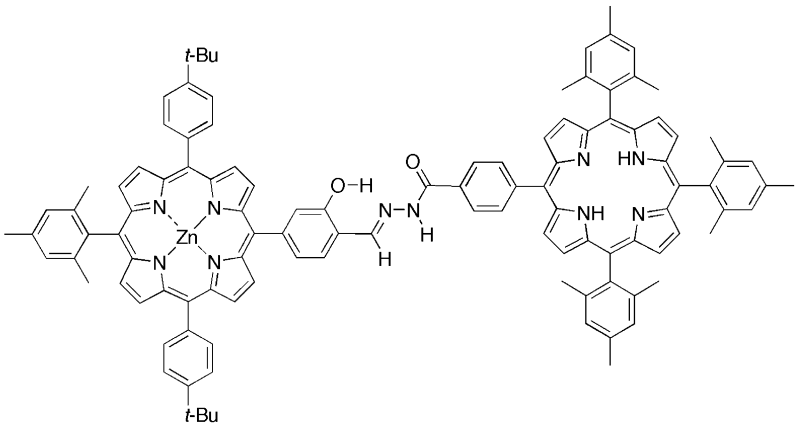

Dyad-3

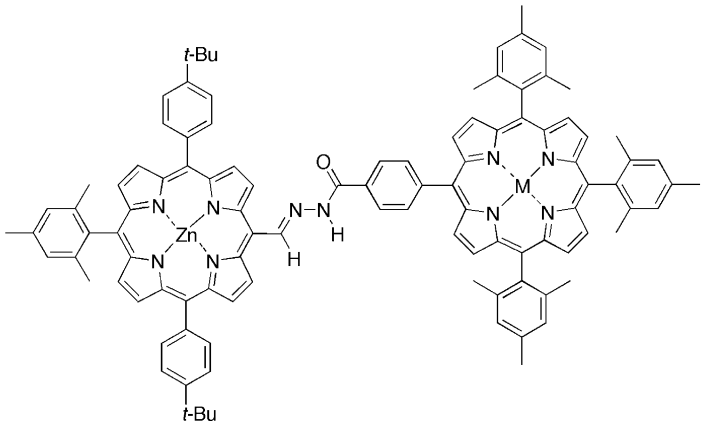

M = H,H **Dyad-4**

M = Zn **Dyad-5**

acac- or imine-linked dyads. We investigated the assembly properties of the building blocks and obtained the imine-linked porphyrin dyads (**Dyads-1**−**5**; Chart 2). We also report the energy-transfer properties of the imine-linked

Chart 3

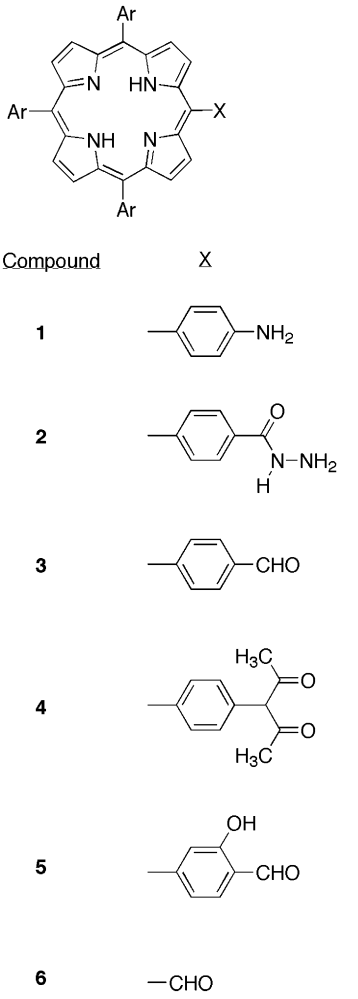

dyads containing a zinc porphyrin and a free base porphyrin, or two zinc porphyrins. In the following paper, we describe the formation and properties of porphyrin-dipyrrin-metal complexes that are also prepared via a self-assembly process.[23]

Results and Discussion

Synthesis. Porphyrin Building Blocks. The porphyrin building blocks for forming self-assembled dyads are shown in Chart 3. Each porphyrin bears one reactive functional group (X) that gives rise to the linker, and three nonlinking substituents (Ar) to provide enhanced solubility in organic solvents. Two common routes were employed for the synthesis of the porphyrins: (1) a mixed-aldehyde condensation with pyrrole followed by functional group manipulations as needed, or (2) attachment of the reactive functional group to the porphyrin nucleus. The mixed-aldehyde route was employed to prepare porphyrins **1**−**4**, while Suzuki coupling or Vilsmeier formylation was employed to prepare porphyrin **5** or **6**, respectively.

A mixed-aldehyde condensation[24] of mesitaldehyde, an aldehyde of choice, and pyrrole in 3:1:4 ratio followed by

Scheme 1

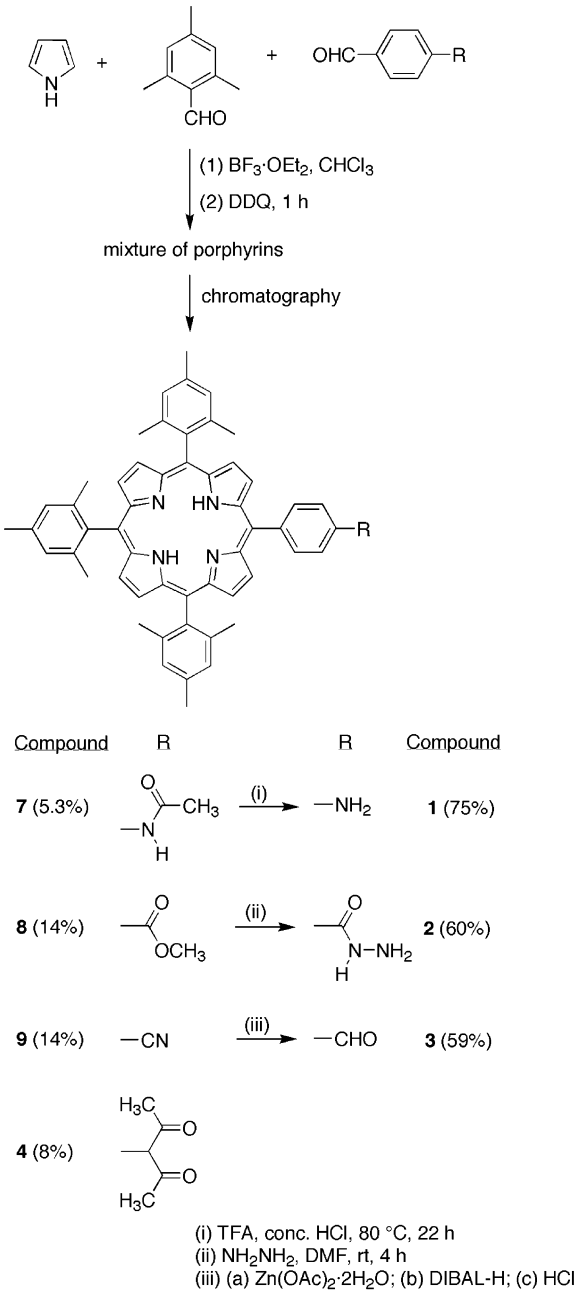

oxidation with 2,3-dichloro-5,6-dicyano-1,4-benzoquinone (DDQ) typically affords a statistical mixture containing six porphyrins. The success of the condensation with mesitaldehyde requires use of BF_3·OEt_2−ethanol cocatalysis conditions, which are achieved by performing the reaction with BF_3·OEt_2 in $CHCl_3$ containing 0.8% ethanol.[25] For aldehydes with at least moderately polar substituents, the desired trimesitylporphyrin is typically the second of the six porphyrins on chromatographic elution. Note that rational methods have not yet been developed that enable the synthesis of porphyrins bearing three mesityl groups.[26]

(23) Yu, L.; Muthukumaran, K.; Sazanovich, I. V.; Kirmaier, C.; Hindin, E.; Diers, J. R.; Boyle, P. D.; Bocian, D. F.; Holten, D.; Lindsey, J. S. *Inorg. Chem.* **2003**, *42*, 6629−6647.

(24) Lindsey, J. S.; Prathapan, S.; Johnson, T. E.; Wagner, R. W. *Tetrahedron* **1994**, *50*, 8941−8968.

(25) Lindsey, J. S.; Wagner, R. W. *J. Org. Chem.* **1989**, *54*, 828−836.

(26) Rao, P. D.; Dhanalekshmi, S.; Littler, B. J.; Lindsey, J. S. *J. Org. Chem.* **2000**, *65*, 7323−7344.

The reaction of mesitaldehyde, pyrrole, and 4-(2,4-dioxopentan-3-yl)benzaldehyde, 4-acetamidobenzaldehyde, methyl 4-formyl benzoate, or 4-cyanobenzaldehyde afforded the corresponding porphyrin bearing three mesityl groups and one acac (**4**), acetamide (**7**), methyl ester (**8**),[24] or nitrile (**9**) group (Scheme 1). Hydrolysis[27] of porphyrin-amide **7** with HCl/trifluoroacetic acid (TFA) at 80 °C gave porphyrin-amine **1** in 75% yield. Treatment of the porphyrin-ester **8** with 98% hydrazine monohydrate in a mixture of THF/EtOH, a 1.0 M solution of hydrazine in THF, or hydrazine in THF did not readily afford the desired porphyrin-hydrazide **2**. However, the reaction of **8** with a 1:3 mixture of hydrazine/DMF[28] gave porphyrin-hydrazide **2** in 60% yield. Reduction of porphyrin-nitrile **9** with diisobutylaluminum hydride (DIBAL-H) gave an aluminum porphyrin. Therefore, free base porphyrin **9** was first metalated with $Zn(OAc)_2 \cdot 2H_2O$, the zinc chelate was reduced with DIBAL-H, and acidic workup gave the free base porphyrin-aldehyde **3**. Porphyrins **2** and **3** were metalated on treatment with $Zn(OAc)_2 \cdot 2H_2O$ to give the zinc chelates **Zn-2** and **Zn-3**.

The synthesis of a porphyrin bearing a meso-salicylaldehyde group (**5**) was pursued by a Suzuki coupling route to avoid the obvious potential complications of condensation of pyrrole with the salicylaldehyde entity. The synthesis of the porphyrin precursor for the Suzuki coupling is shown in Scheme 2. The known diacyldipyrromethane **10**[26] was reduced with $NaBH_4$ in THF/methanol (10:1), affording the corresponding dicarbinol **10-diol**. The latter was condensed with dipyrromethane (**11**)[29] under new catalysis conditions ($InCl_3$ in CH_2Cl_2 at room temperature)[30] followed by oxidation with DDQ, affording the porphyrin bearing one unsubstituted meso-position (**12**) in 19% yield. No other porphyrins were observed in this reaction.

Therien et al. have reported a number of Suzuki couplings with zinc porphyrins bearing meso-bromo groups.[31] Bromination of **12** at the unsubstituted meso-position in a standard method[32] by treatment with *N*-bromosuccinimide (NBS) in $CHCl_3$ in the presence of pyridine gave bromo-porphyrin **13**, which was metalated with $Zn(OAc)_2 \cdot 2H_2O$ to give **Zn-13**. Suzuki coupling of **Zn-13** with pinacolborane under Pd-$(PPh_3)_2Cl_2$ catalysis in dichloroethane at 90 °C provided dioxaborolane-porphyrin **Zn-14** in 89% yield.

The catalytic system reported to give the highest activity for Suzuki reactions with 5-bromosalicylaldehyde derivatives employs a palladium reagent ($Pd(dppf)Cl_2$ or $Pd(PPh_3)_4$) and

Scheme 2

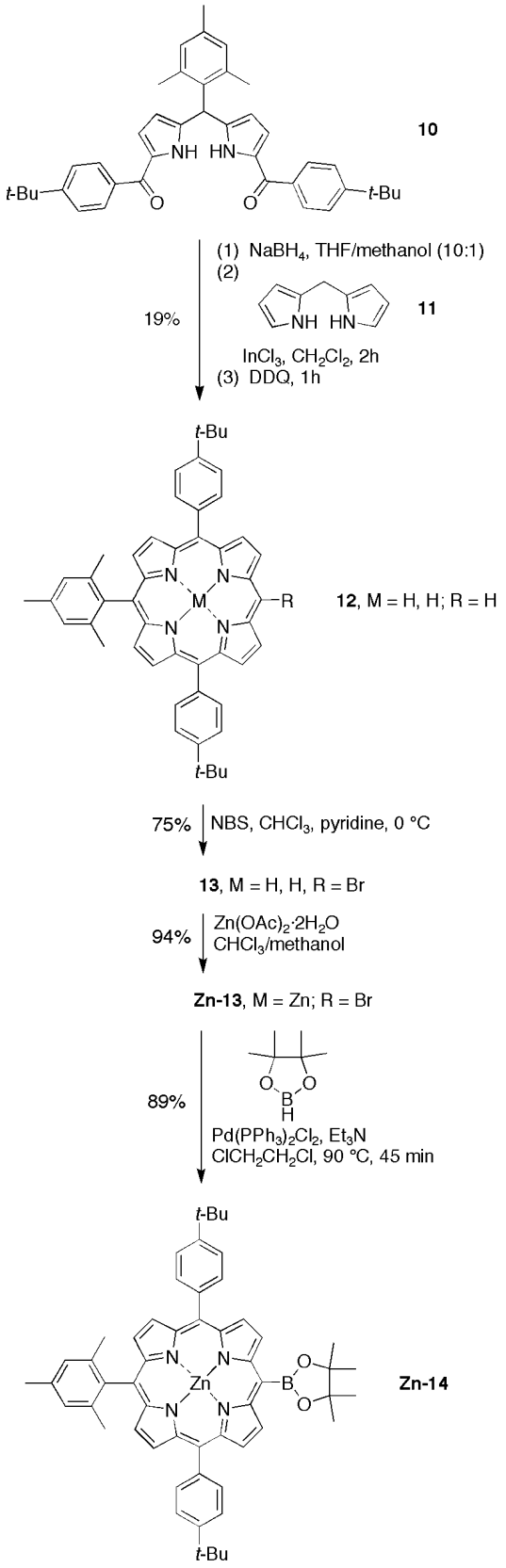

K_2CO_3 in dimethoxyethane (DME)/H_2O (3:1).[33] The reaction of **Zn-14** and 4-bromosalicylaldehyde (**15**; prepared by Reimer−Tiemann formylation of 3-bromophenol;[34] see Supporting Information) under these conditions at 90 °C for 3 h

(27) Lindsey, J. S.; Brown, P. A.; Siesel, D. A. *Tetrahedron* **1989**, *45*, 4845−4866.
(28) Nutt, R. F.; Veber, D. F.; Saperstein, R. *J. Am. Chem. Soc.* **1980**, *102*, 6539−6545.
(29) (a) Littler, B. J.; Miller, M. A.; Hung, C.-H.; Wagner, R. W.; O'Shea, D. F.; Boyle, P. D.; Lindsey, J. S. *J. Org. Chem.* **1999**, *64*, 1391−1396. (b) Wang, Q. M.; Bruce, D. W. *Synlett* **1995**, 1267−1268.
(30) Geier, G. R., III; Callinan, J. B.; Rao, P. D.; Lindsey, J. S. *J. Porphyrins Phthalocyanines* **2001**, *5*, 810−823.
(31) Hyslop, A. G.; Kellett, M. A.; Iovine, P. M.; Therien, M. J. *J. Am. Chem. Soc.* **1998**, *120*, 12676−12677.
(32) DiMagno, S. G.; Lin, V. S.-Y.; Therien, M. J. *J. Org. Chem.* **1993**, *58*, 5983−5993.
(33) (a) Morris, G. A.; Nguyen, S. T. *Tetrahedron Lett.* **2001**, *42*, 2093−2096. (b) Zhuravel, M. A.; Nguyen, S. T. *Tetrahedron Lett.* **2001**, *42*, 7925−7928.

Scheme 3

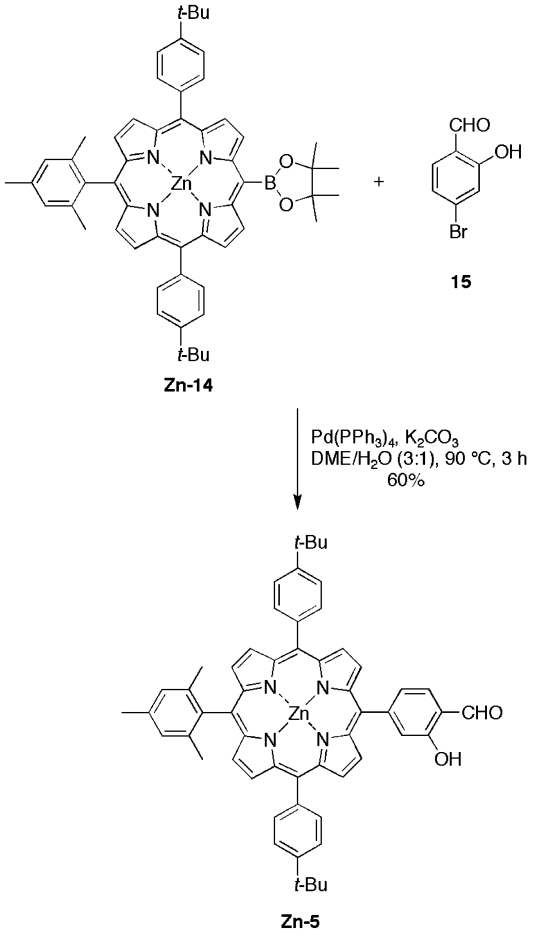

gave the desired porphyrin-salicylaldehyde **Zn-5** in 60% yield (Scheme 3).

The porphyrin bearing a meso-formyl group was synthesized as shown in Scheme 4. Conversion of porphyrin **12** to the copper chelate followed by Vilsmeier formylation gave the meso-formyl copper porphyrin **Cu-6** in 80% yield. Demetalation with TFA/H_2SO_4 afforded porphyrin **6** in 62% yield; subsequent metalation with $Zn(OAc)_2 \cdot 2H_2O$ gave the zinc porphyrin (**Zn-6**) in 92% yield.

Self-Assembled Dyads. Treatment of the free base porphyrin-acac (**4**) with $Zn(OAc)_2 \cdot 2H_2O$ resulted in formation of an unknown product rather than the expected self-assembled bis(zinc-porphyrin-acac)Zn(II) dimer (see Supporting Information). We turned our attention to the imine-linked dyads. Imines derived from small molecules are typically formed by treating an aldehyde and an amine at high concentration in a suitable solvent (preferably alcoholic solvents) or in refluxing benzene or toluene under acid catalysis with azeotropic removal of water.[35] Such conditions are not applicable for preparing **Dyads-1**−**5** for two reasons. (1) High concentrations are not readily achieved with porphyrins. (2) Strong acids cause demetalation of zinc porphyrins. Accordingly, a solution of amino-porphyrin **1** and aldehyde-porphyrin **Zn-5** (5 mM each) in THF/EtOH

Scheme 4

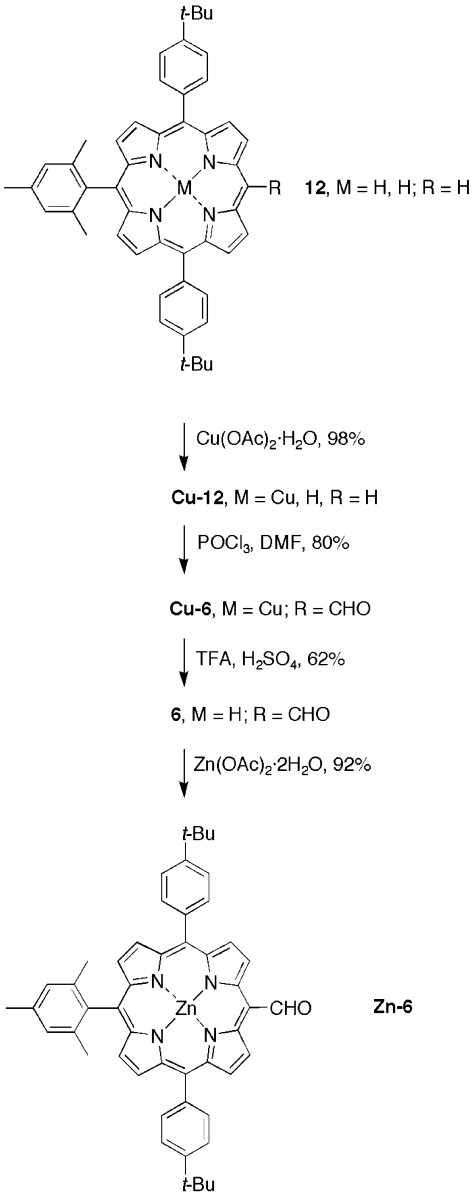

(3:1) was stirred at room temperature in the absence of acid catalysis. After 40 h, the analytical size exclusion chromatography (SEC) showed only ∼15% yield of the imine-dyad product (**Dyad-1**). Next, reactions were performed with attempted catalysis by $Yb(OTf)_3$ or $Dy(OTf)_3$ (1.0−3.2 mM) in THF. Such catalysts were chosen because earlier studies showed that zinc porphyrins are quite stable upon exposure to these lanthanide triflates.[36] Yields of 30−40% were obtained upon reaction for 18−22 h.

The reaction of **Zn-5** and **1** (5.0 mM each) in the presence of $Yb(OTf)_3$ (1.0 mM) in THF at room temperature for 5 h afforded **Dyad-1** in 38% yield (Chart 2). The analytical SEC

(34) (a) Kobayashi, S.; Azekawa, M.; Morita, H. *Chem. Pharm. Bull*. **1969**, *17*, 89−93. (b) Glennon, R. A.; McKenney, J. D.; Lyon, R. A.; Titeler, M. *J. Med. Chem.* **1986**, *29*, 194−199.

(35) (a) Houjou, H.; Lee, S.-K.; Hishikawa, Y.; Nagawa, Y.; Hiratani, K. *Chem. Commun.* **2000**, 2197−2198. (b) Muñoz-Hernández, M.-A.; Keizer, T. S.; Parkin, S.; Patrick, B.; Atwood, D. A. *Organometallics* **2000**, *19*, 4416−4421. (c) Roesch, K. R.; Larock, R. C. *J. Org. Chem.* **2001**, *66*, 412−420. (d) Bachmann, S.; Furler, M.; Mezzetti, A. *Organometallics* **2001**, *20*, 2102−2108.

(36) Speckbacher, M.; Yu, L.; Lindsey, J. S. *Inorg. Chem.* **2003**, *42*, 4322−4337.

Chart 4

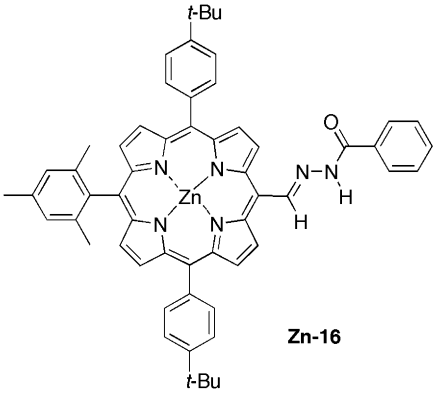

Zn-16

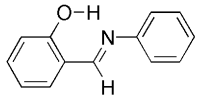

17

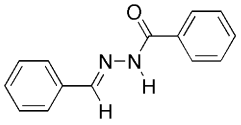

18

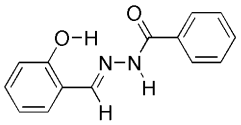

19

of aliquots from the reaction mixture of the dyad-forming reactions showed two sharp peaks with a difference in retention times of ~0.7 min, corresponding to the dyad and the two monomers (the latter co-chromatographed with each other). **Dyads-2**−**5** were each prepared in similar fashion in yields of 30−60%.

Benchmarks. For comparison purposes, we prepared the benchmarks shown in Chart 4. Porphyrin **Zn-16** contains the same linker present in **Dyad-5**. A reaction of 5.0 mM each of **Zn-6** and benzoic hydrazide in the presence of $Yb(OTf)_3$ (1.0 mM) in THF at room temperature for 46 h afforded porphyrin **Zn-16** in 70% isolated yield. Variable temperature ^{1}H NMR experiments of **Zn-16** revealed the presence of two interconverting conformers (see below). The small molecules **17**,[37] **18**,[38] and **19**[38] represent the linkers. These were prepared in quantitative yield by mixing the respective aldehyde with the amino compound under neat conditions. Compound **17** is yellow while **18** and **19** are colorless. The absorption spectrum in CH_3CN at room temperature of **17**, **18**, or **19** showed a broad, long-wavelength absorption band with a peak position of 336, 293, or 325 nm, respectively.

Chemical Characterization. Each dyad was characterized by analytical SEC, LD-MS, and ^{1}H NMR, IR, absorption, and fluorescence spectroscopy. Each of the purified dyads showed a single component by TLC and a single peak by analytical SEC. The dyads were quite stable toward routine handling over a period of days in nonpolar or polar solvents or in the solid state (see Supporting Information).

The absorption spectrum of **Dyads-1**−**4** showed the presence of the zinc and free base porphyrins. The fluorescence spectra are described below. The IR spectra show negligible (for **Dyad-1**) or weak (for dyads **Dyad-2**−**5**) IR absorption in the 3200−3400 cm^{-1} region (characteristic of the N−H stretch) and intense bands in the region 1590−1670 cm^{-1} (characteristic of C═N and/or C═O signals). Each of the dyads was examined by ^{1}H NMR spectroscopy. The ^{1}H NMR spectra of **Dyad-1** and **Dyad-3** (containing the salicylaldimine unit) were unremarkable, generally showing sharp lines and the superposition of the spectra derived from the porphyrin entities of the component parts except for the expected changes owing to the formation of the imine linkage. The ^{1}H NMR spectra at room temperature of **Dyad-2**, **Dyad-4**, and the benchmark **Zn-16** each showed evidence of two conformers in 8:1, 6:1, and 6:1 ratio, respectively (**Dyad-5** gave a poor quality spectrum). The diagnostic for the occurrence of conformers is the presence of two singlets stemming from the NH proton, and for **Dyads-4**−**5** and **Zn-16**, from the two singlets for the imine CH proton and the two sets of peaks for the β-pyrrole protons flanking the imine. The identity of the NH proton signal was confirmed by D_2O exchange. Compound **18**, which represents the acyl hydrazone linker alone, also exhibited two conformers in 10:1 ratio. The small amount of minor conformer of the same compound was not detected in a much earlier NMR study.[39] Variable-temperature ^{1}H NMR experiments (400 MHz) of **Dyad-2**, **Dyad-4**, and **Zn-16** established the slow interconversion of the conformers on the NMR time scale (see Supporting Information).

Each compound wherein two conformers were observed (**Dyad-2**, **Dyad-4**, **Zn-16**) contains an acyl hydrazone linker derived from an aldehyde lacking the *o*-hydroxy group. Conformational isomerism in acyl hydrazones is well established.[40] The acyl hydrazone motif presents two sites for conformational isomerism: the *cis*/*trans* amide and the *E*/*Z* imine. Multiple conformers were not observed for the salicylaldehyde-derived dyads, regardless of whether the linkage is an imine or an acyl hydrazone (i.e., **Dyad-1**, **Dyad-3**). In each case, the major conformer constitutes at least 85% of the total and is assumed to be the *trans*-*E* conformer as displayed in Charts 1 and 2. Observation of conformers in all compounds lacking the stabilizing *o*-hydroxy group, and no conformers in those containing the *o*-hydroxy group, is consistent with isomerism about the imine rather than the amide unit.

Physical Studies. In the following, the properties of each of the dyads and reference compounds are described, with results for **Dyad-3** selected as generally exemplary for **Dyads-1**−**3**. Additional data for each dyad (and reference compounds) are given in the Supporting Information. For

(37) Steevens, J. B.; Pandit, U. K. *Tetrahedron* **1983**, *39*, 1395−1400.
(38) Struve, G. *J. Prakt. Chem.* **1894**, *50*, 295−310.
(39) Palla, G.; Pelizzi, C.; Predieri, G.; Vignali, C. *Gazz. Chim. Ital.* **1982**, *112*, 339−341.
(40) Pihlaja, K.; Simeonov, M. F.; Fülöp, F. *J. Org. Chem.* **1997**, *62*, 5080−5088.

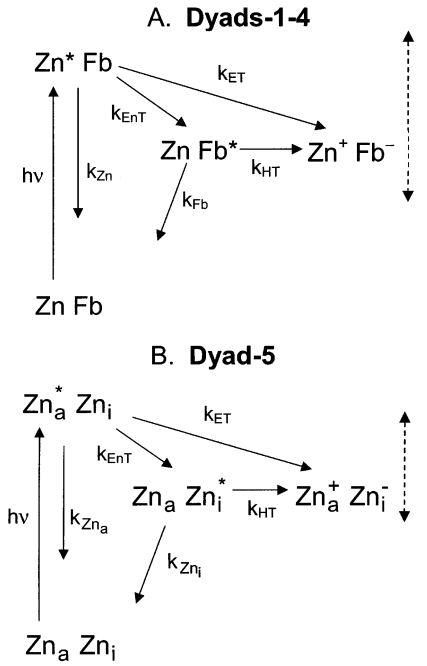

Figure 1. Schematic state diagram showing the likely excited-state processes in the dyads, which include energy transfer (EnT), electron transfer (ET), and hole transfer (HT). The processes labeled k_{Zn} and k_{Fb} include the intrinsic decay processes (fluorescence and internal conversion to the ground-state plus intersystem crossing to the excited triplet state) for the respective Zn* and Fb* excited states. The dashed arrows indicate that the (free) energies of the charge-separated states depend on dyad and medium. In part B, Zn_i and Zn_a represent the imine- and aryl-substituted zinc porphyrins, respectively.

Table 1. Half-Wave Potentials (V) of the Benchmark Zn Porphyrins[a]

porphyrin	$E^{0/+1}$	$E^{+1/+2}$	$E^{+2/+3}$	$E^{+3/+4}$
Zn-3	0.60	0.91	*b*	*b*
Zn-5	0.60	0.91	*b*	*b*
Zn-6	0.75	0.96	*b*	*b*
Zn-16	0.55	0.87	1.00	1.26

[a] Potentials were obtained in CH_2Cl_2 containing 0.1 M Bu_4NPF_6. *E*-values reported vs Ag/Ag^+, $FeCp^2/FeCp^{2+}$ = 0.19 V, and scan rate = 0.1 V s^{-1}. Values are ± 0.03 V. [b] Not observed.

convenience in presenting the results, the relevant excited-state processes in the dyads are illustrated in Figure 1.

Electrochemistry. To examine the effects of the linker on the ground-state electronic properties of the porphyrins, we investigated the redox properties of the benchmark zinc porphyrins **Zn-3**, **Zn-5**, **Zn-6**, and **Zn-16** in the 0−1.5 V range using both square-wave and cyclic voltammetry. In this window, all four porphyrins exhibited reversible and reproducible voltammetry. The redox potentials are summarized in Table 1. **Zn-3**, **Zn-5**, and **Zn-6** each exhibit two oxidation waves in the 0−1.5 V range, as typically found for Zn porphyrins.[41] The potentials for **Zn-3** and **Zn-5** are identical ($E^{0/+1}$ = 0.60) and somewhat more positive than those observed for either *meso*-tetraphenylporphinatozinc(II) (ZnTPP, $E^{0/+1}$ = 0.56 V) or *meso*-tetramesitylporphinatozinc(II) (ZnTMP, $E^{0/+1}$ = 0.51 V).[42] These results indicate

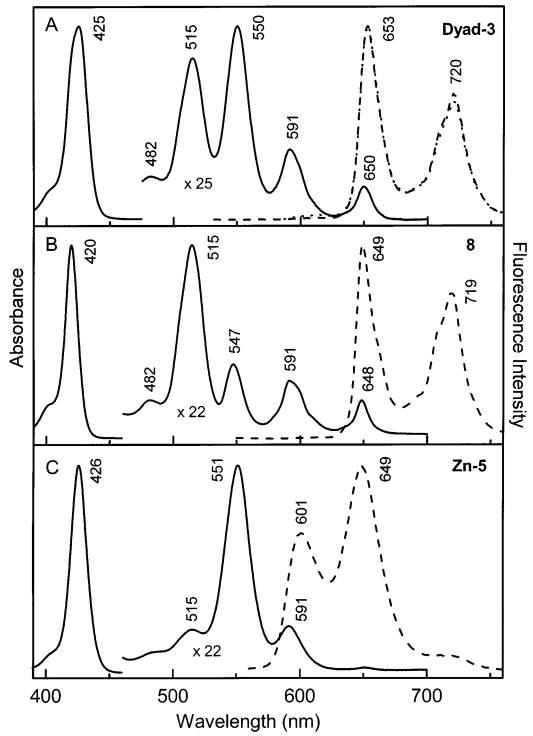

Figure 2. Electronic absorption spectra (—) and fluorescence spectra (− − and · · ·) for **Dyad-3** (A) and the reference compounds **8** (B) and **Zn-5** (C) in toluene at room temperature. Absorption data between 470 and 700 nm have been multiplied by the factors shown. Dyad emission in part A was obtained using predominant excitation of the free base porphyrin at 517 nm (− −) or zinc porphyrin at 565 nm (· · ·). Spectra in the respective regions have been normalized to the same peak intensity, and the maxima (±1 nm) indicated.

that (1) the meta-hydroxy group has no measurable effect on the ground-state electronic properties of the porphyrin and (2) the *para*-aldehyde exerts a modest electron-withdrawing effect. The redox waves for **Zn-6** ($E^{0/+1}$ = 0.75 V) are considerably more positive and reflect the substantial electron-withdrawing effects of the aldehyde directly attached to the meso-position of the porphyrin ring.

The redox characteristics of **Zn-16** are unusual in two aspects. (1) The complex exhibits four waves in the 0−1.5 V range (Table 1) instead of two. Two of these waves are in a range typical of Zn porphyrins (<1 V), whereas two are at higher potentials (>1 V). To ensure that the additional waves were not due to aggregation (or other undetermined effects), the redox characteristics of the complex were examined after multiple dilutions of the original sample. In all cases, the voltammetric characteristics were reproducible under conditions of multiple redox cycling. Consequently, the additional voltammetric waves must reflect the participation of the appended imine group. (2) The potential of the first redox wave of **Zn-16** ($E^{0/+1}$ = 0.55 V) is not appreciably different from that of ZnTPP or ZnTMP despite the fact that the imine moiety appended at the porphyrin meso-position can potentially conjugate with the porphyrin π-system. Accordingly, these results suggest that the imine group is not appreciably conjugated in the ground electronic state of the complex.

Absorption Spectra. The electronic ground-state absorption spectrum of ZnFb array **Dyad-3** and its constituent parts

(41) Felton, R. H. In *The Porphyrins*; Dolphin, D., Ed.; Academic Press: New York, 1978; Vol. 5, pp 53−125.
(42) Loewe, R. S.; Lammi, R. K.; Diers, J. R.; Kirmaier, C.; Bocian, D. F.; Holten, D.; Lindsey, J. S. *J. Mater. Chem.* **2002**, *12*, 1530−1552.

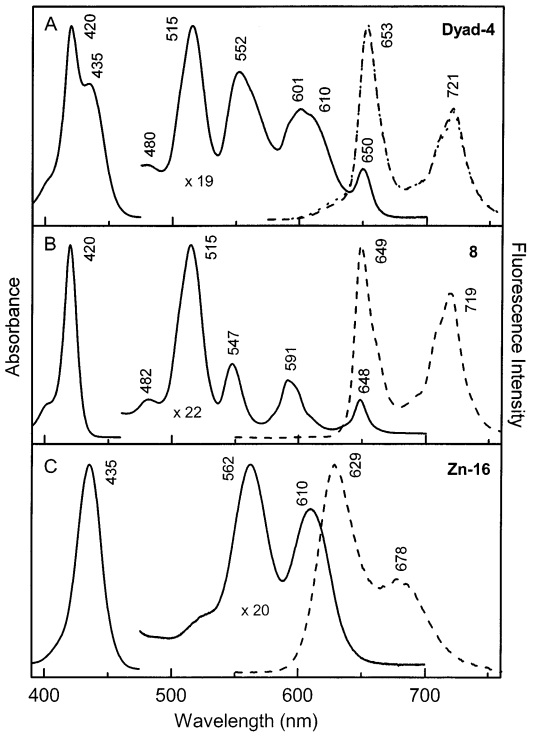

Figure 3. Electronic absorption spectra (—) and fluorescence spectra (– – and · · ·) for **Dyad-4** (A) and the reference compounds **8** (B) and **Zn-16** (C) in toluene. Other details are the same as those for Figure 2.

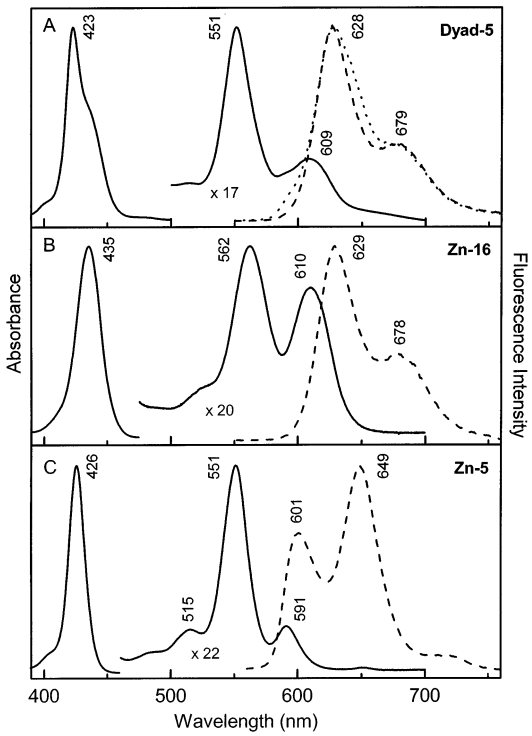

Figure 4. Electronic absorption spectra (—) and fluorescence spectra (– – and · · ·) for **Dyad-5** (A) and the reference compounds **Zn-16** (B) and **Zn-5** (C) in toluene. Dyad emission in part A was obtained using predominant excitation of the imine-substituted zinc porphyrin at 438 nm (– –) or the aryl-substituted zinc porphyrin at 423 (· · ·). Other details are the same as those for Figure 2.

(zinc porphyrin **Zn-5** and free base porphyrin **8)** are shown in Figure 2. Superposition of the absorptions of the zinc and free base reference compounds affords a first-order representation of the spectrum of **Dyad-3**. This is especially true in the visible Q-band ($S_0 \rightarrow S_1$) region (480−650 nm), whereas the spectrum in the Soret region (420−425 nm) likely also contains effects (shifts/splittings) due to exciton coupling of the strong B transition dipoles of the subunits. A similar analysis applies to **Dyad-1** and **Dyad-2** in toluene. The absorption spectra of **Dyads-1**−**3** in benzonitrile are also a close composite of the associated reference spectra, all displaying the typical red shifts and intensity-ratio changes due to solvent coordination to the metal ion of the zinc porphyrin subunit. These findings, the redox data described above, and the emission results described below indicate that the inter-porphyrin electronic interactions mediated by the linker motifs employed in **Dyads-1**−**3** do not significantly perturb the electronic properties of the porphyrin subunits in the ground state or photophysically relevant S_1 excited state compared to the isolated pigments. We have drawn similar conclusions previously for ZnFb dyads employing diarylethyne, diphenylbutadiyne, and *p*-phenylene linkers.[43]

Figure 3 shows absorption spectra of **Dyad-4** and its reference compounds **Zn-16** and **8** in toluene. The zinc porphyrin component of **Dyad-4** (and **Zn-16**) contains the imine group of the linker attached directly to the macrocycle whereas a mediating aryl ring is present in **Dyads-1**−**3** (and **Zn-5**). This direct attachment in **Zn-16** and **Dyad-4** results in red shifted and broader absorption bands with an altered Q-band intensity ratio (Figure 3 versus Figure 2). The finding that a meso-imine group lowers the energy of the S_1 excited state of zinc porphyrin **Zn-16** relative to analogues such as **Zn-5** prompted us to prepare **Dyad-5**, which contains two, inequivalent zinc porphyrins (Chart 2). The spectrum of this dyad (Figure 4) is again well approximated by the superimposed reference spectra. The excited-state energies implied by the absorption spectra in Figures 3 and 4 (and the fluorescence spectra given below) indicate that the imine-substituted zinc porphyrin (Zn_i) should serve as the energy-transfer *donor* to the free base porphyrin in **Dyad-4** whereas it should be the energy-transfer *acceptor* from the aryl-substituted zinc porphyrin (Zn_a) in **Dyad-5**, as shown in Figure 1. This reversed direction of excited-state energy flow is indeed found in the studies described below.

Fluorescence Spectra and Quantum Yields. Emission profiles for **Dyad-3** and reference porphyrins **8** and **Zn-5** in toluene are shown in Figure 2 (dashed and dotted spectra). The emission spectra of **Dyad-3** (Figure 2A) clearly show that the fluorescence occurs essentially exclusively from the free base porphyrin moiety, with perhaps trace emission from the zinc porphyrin component (e.g., near 600 nm). This is true for both excitation of (predominantly) the free base porphyrin subunit at 517 nm (– –) or the zinc porphyrin

(43) (a) Hsiao, J.-S.; Krueger, B. P.; Wagner, R. W.; Johnson, T. E.; Delaney, J. K.; Mauzerall, D. C.; Fleming, G. R.; Lindsey, J. S.; Bocian, D. F.; Donohoe, R. J. *J. Am. Chem. Soc.* **1996**, *118*, 11181−11193. (b) Li, F.; Gentemann, S.; Kalsbeck, W. A.; Seth, J.; Lindsey, J. S.; Holten, D.; Bocian, D. F. *J. Mater. Chem.* **1997**, *7*, 1245−1262. (c) Youngblood, W. J.; Gryko, D. T.; Lammi, R. K.; Bocian, D. F.; Holten, D.; Lindsey, J. S. *J. Org. Chem.* **2002**, *67*, 2111−2117. (d) Yang, S. I.; Li, J.; Cho, H. S.; Kim, D.; Bocian, D. F.; Holten, D.; Lindsey, J. S. *J. Mater. Chem.* **2000**, *10*, 283−296.

Table 2. Photophysical Properties of Dyads and Reference Compounds[a]

		excited-state lifetime (ps)[b]		fluorescence yield					
compd	solvent	Zn*	Fb*	Zn* [c]	Fb* [d]	$(k_{EnT})^{-1}$ (ps)[e]	Φ_{EnT}[f]	Φ_{ET}[g]	Φ_{HT}[h]
				Dyads					
Dyad-1	toluene	13 ± 2	12500		0.13 (0.13)	13	0.99	≤0.01	0.06
	benzonitrile		10400		0.12 (0.11)		>0.9	<0.1	0.23
Dyad-2	toluene	65 ± 10	12300		0.11 (0.12)	67	0.97	≤0.03	0.08
	benzonitrile		11000		0.11 (0.11)		>0.9	<0.1	0.19
Dyad-3	toluene	68 ± 4	12800		0.13 (0.16)	70	0.97	≤0.03	0.04
	benzonitrile		10400		0.10 (0.093)		>0.9	<0.1	0.23
Dyad-4	toluene	5.4 ± 0.7	11100		0.13 (0.13)	8.3	0.65	0.35	0.18
	benzonitrile	3.0 ± 0.3	4200		0.10 (0.10)	6.0	0.50	0.50	0.61
Dyad-5	toluene	2.5 ± 0.2[i]		0.072		3.1[k]	>0.8	≤0.2	0.10
		1900[j]		(0.058)					
	benzonitrile	1600[j]							0.11
				Monomers[l]					
8	toluene		13300		0.11				
	benzonitrile		13500		0.13				
Zn-5	toluene	2200		0.040					
	benzonitrile	1800		0.043					
Zn-16	toluene	2100		0.049					
	benzonitrile	1800		0.046					

[a] All data were taken at room temperature. [b] Lifetime of the lowest excited state. For Zn porphyrin energy-transfer donors in the dyads, lifetimes were determined using transient absorption data; for the energy-accepting free base porphyrin in **Dyads-1**−**4** and imine-substituted zinc porphyrin in **Dyad-5**, and for the reference compounds, the lifetimes (±5%) were measured by fluorescence modulation (phase shift) spectroscopy using nitrogen-purged samples. [c] Fluorescence yield (±15%) of the zinc porphyrins (in the presence of dissolved oxygen of air) relative to ZnTPP in toluene ($\Phi_f = 0.030$)[46] obtained using excitation for **Dyad-5** (toluene) of the imine-substitututed zinc porphyrin at 437 nm or the aryl-substituted zinc porphyrin at 423 nm (value in parentheses), **Zn-5** at 550 nm (toluene) or 380 nm (benzonitrile), or **Zn-16** at 400 nm (both solvents). [d] Fluorescence yield (±10%) of the free base porphyrins (in the presence of dissolved oxygen of air) relative to (free base) *meso*-tetraphenylporphyrin in toluene ($\Phi_f = 0.11$)[46] obtained with predominant excitation of this moiety at 517 nm for **Dyads-1**−**4** and 515 nm for **8**. The value in parentheses for each dyad is the Fb* fluorescence yield obtained with predominant excitation of the zinc porphyrin at 565 nm. [e] Inverse of the rate constant for Zn*Fb → ZnFb* energy transfer (**Dyads-1**−**4**) or Zn_a*Zn_i → Zn_aZn_i* energy transfer (**Dyad-5**). [f] Quantum yield of Zn*Fb → ZnFb* or Zn_a*Zn_i → Zn_aZn_i* energy transfer. [g] Quantum yield of Zn*Fb → Zn^+Fb^- or ZnZn* → Zn^+Zn^- electron transfer. [h] Quantum yield of ZnFb* → Zn^+Fb^- hole transfer for **Dyads-1**−**4** and for ZnZn* → Zn^+Zn^- transfer in **Dyad-5** obtained from the excited-state lifetimes. These values are considered to be upper limits since the yields calculated from the fluorescence yields are somewhat less. [i] Zn* lifetime of the aryl-substituted zinc porphyrin energy-transfer donor. [j] Zn* lifetime of the imine-substituted zinc porphyrin energy-transfer acceptor. [k] Calculated assuming $\Phi_{EnT} = 0.8$. The value is in the range $(2.5-3.1\ ps)^{-1}$. [l] The values for the reference compounds are similar to those obtained previously for other zinc and free base reference porphyrins.[47]

component at 565 nm (···). Furthermore, the yield of emission from the free base porphyrin in **Dyad-3** in toluene (using excitation of either porphyrin) is comparable to that of reference compound **8** (Table 2). These combined results for **Dyad-3** in toluene indicate (1) very efficient Zn*Fb → ZnFb* energy transfer (>95%) with little yield of competing Zn*Fb → Zn^+Fb^- electron transfer, and (2) virtually no subsequent quenching of ZnFb* via ZnFb* → Zn^+Fb^- hole transfer (Figure 1). Basically, the same emission spectra and fluorescence yields are obtained for **Dyad-1** and **Dyad-2** in toluene (Table 2).

Generally similar results are also found for **Dyads-1**−**3** and reference compounds **Zn-5** and **8** in benzonitrile (Table 2). Again, emission from the dyads occurs primarily from the free base porphyrin moiety upon excitation of either subunit. However, the Fb* emission yields for the dyads are modestly reduced (up to ∼30%, using excitation of either component) compared to the fluorescence yield of **8** in benzonitrile. Thus, although Zn*Fb → ZnFb* energy transfer remains efficient for **Dyads-1**−**3** in the polar solvent, the reduced fluorescence yield indicates that Fb* is modestly quenched by hole transfer (Figure 1).

Figures 3 and 4 show the emission profiles for ZnFb **Dyad-4** and ZnZn **Dyad 5**, respectively, and their reference components in toluene. Several points regarding the emission spectrum of **Zn-16** are noteworthy. First, the emission bands of **Zn-16** do not obey the (normal) approximate absorption/fluoresence mirror symmetry relationship of zinc porphyrins, such as exhibited by **Zn-5**. Second, there is a larger Stokes shift between the Q(0,0) absorption and emission maxima (∼19 nm; ∼495 cm^{-1}) for **Zn-16** than for **Zn-5** (∼10 nm; ∼280 cm^{-1}) or Fb porphyrin **8** (∼1 nm; ∼25 cm^{-1}). These results likely reflect photoinduced reorientations that increase conjugation between the porphyrin and imine units. Note that **Dyad-4**, **Dyad-5**, and **Zn-16** each contain the meso-linked acyl hydrazone linker, which gives two conformers. That these effects occur mainly in the excited state and not the ground state is indicated by the similar redox potentials of **Zn-16** and **Zn-5** (Table 1). Analogous results are found for **Dyad-4**, **Dyad-5**, and **Zn-16** in benzonitrile (where, additionally, the absorption and emission bands are red-shifted due to solvent ligation to the zinc). The fluorescence yields for **Zn-16** in toluene and benzonitrile are comparable to those for **Zn-5** (and related benchmark porphyrins), as are the Zn* lifetimes described below (Table 2).

The emission from **Dyad-4** (like **Dyads-1**−**3**) occurs primarily from the free base porphyrin, using excitation of either subunit and for both toluene (Figure 3A) or benzonitrile. Similarly, in toluene the Fb* emission yield for **Dyad-4** is comparable to **8** and is reduced only slightly in benzonitrile (again using excitation of either component).

In the ZnZn **Dyad-5**, the imine-substituted zinc porphyrin (Zn_i) is the lower energy of the two chromophores, opposite to the situation for ZnFb **Dyad-4** as noted above. Conse-

quently, emission from **Dyad-5** occurs primarily from Zn_i* (Figure 4A). The integrated amplitude of this emission using Soret excitation of the aryl-substituted porphyrin (Zn_a) is about 20% lower than that obtained using Soret excitation of Zn_i (after correction for absorbance at λ_{ex} and residual emission from Zn_a). On the basis of these results, we estimate that Zn_a*$Zn_i \rightarrow Zn_aZn_i$* energy transfer has a yield of $\geq$80% for **Dyad-5** in toluene (Figure 1 and Table 2).

Fluorescence Lifetimes. The excited-state lifetimes for the free base porphyrin moiety of **Dyads-1**−**4** in both toluene and benzonitrile are given in Table 2 along with the lifetimes for the reference compounds. The yields of ZnFb* $\rightarrow Zn^+Fb^-$ hole transfer in **Dyads-1**−**4** were calculated from these lifetimes using the formula $\Phi_{HT} = 1 - (\tau_{dyad}^{Fb*}/\tau_{ref}^{Fb*})$ and are given in the last column of Table 2. The Fb* lifetimes for **Dyads-1**−**3** in toluene (12−13 ns) are comparable to the reference values (slightly over 13 ns), consistent with the similar emission yields, indicating minimal Fb* quenching by hole transfer. The yield increases to $\Phi_{HT} \sim 0.2$ for **Dyads-1**−**3** in benzonitrile on the basis of a small reduction in Fb* lifetime compared to that in **8** (paralleling the reduction in fluorescence yield). For **Dyad-4**, the Fb* lifetime is slightly quenched in toluene (~11 ns versus ~13 ns; Φ_{HT} ~0.2) and more so in benzonitrile (4.2 ns versus 13.5 ns; Φ_{HT} ~0.6).

A similar analysis for **Dyad-5** gives the yield of Zn_aZn_i* $\rightarrow Zn_a^+Zn_i^-$ hole transfer (Figure 1B). The Zn* lifetime for this dyad in toluene of 1.9 ns presumably derives mainly from Zn_i* (the lower-energy unit). This lifetime is only slightly shorter than that of 2.1 ns for imine-substituted reference porphyrin **Zn-16** and gives $\Phi_{HT} \sim 0.1$; similar results are found in benzonitrile (Table 2). The lower hole-transfer yields for **Dyad-5** compared to **Dyad-4** no doubt derive from $Zn_a^+Zn_i^-$ in the former being at higher energy than Zn^+Fb^- in the latter.

Transient Absorption Spectra and Kinetics. All the dyads were examined by time-resolved absorption difference spectroscopy to obtain the rate constant and yield for Zn*Fb $\rightarrow$ ZnFb* or Zn*Zn $\rightarrow$ ZnZn* energy transfer and to assess the contribution of competing electron transfer (Figure 1). The data were analyzed in the same fashion as we have previously described for other porphyrin-based arrays.[43,44] Representative data for **Dyad-3** and **Dyad-4** in toluene are briefly described (Figures 5 and 6) and differences for the other dyads and solvents highlighted. The measured Zn* lifetimes and calculated rate constants are listed in Table 2.

Dyads-1−**3 in Toluene.** The absorption difference spectrum observed at 0.5 ps after excitation of **Dyad-3** in toluene (Figure 5A, —) is ascribed principally to Zn*, with a minor contribution of Fb* (due to direct excitation of the latter). By 270 ps (− −), the free base bleaching at 515 nm has increased substantially, resulting from the Zn*Fb $\rightarrow$ ZnFb* energy-transfer process. Subsequently, the spectrum shows little change to 3 ns (· · ·), consistent with the Fb* (fluorescence) lifetime of ~13 ns (Table 2) and the minor spectral changes that accompany Fb* decay, which primarily involves formation of the excited triplet state Fb^T (70−80% yield in the isolated pigment[45]).

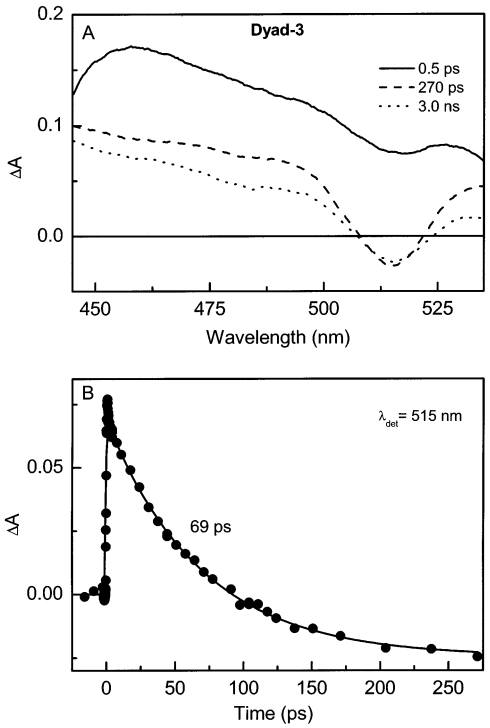

Figure 5. Representative time-resolved absorption spectra (A) and kinetic profile (B) for **Dyad-3** in toluene at room temperature using predominant excitation of the zinc porphyrin component with a 551 nm 130 fs flash. The fit to the kinetic data at 515 nm in part B gives a dominant component with a time constant of 69 ps and a minor ~1 ps phase. The average value for the dominant component reflecting the Zn* lifetime from measurements at several detection wavelengths is given in Table 2.

Figure 5B shows a kinetic profile for the decay of the Zn* excited-state absorption and the formation of the Fb* bleaching at 515 nm (•) for **Dyad-3** in toluene. Also shown is a fit to a dual-exponential function (convolved with an instrument response) plus a constant (for Fb* and Fb^T) affording a dominant (>90%) kinetic component having time constant of 69 ± 4 ps and a minor 1.1 ± 0.3 ps component that may represent some vibrational relaxation of Zn*. Analysis of kinetic traces at a number of wavelengths gives a time constant for the main component of 68 ± 4 ps, which is assigned as the Zn* lifetime for **Dyad-3** in toluene (Table 2). Virtually the same Zn* lifetime (65 ± 10 ps) is found for **Dyad-2**, which is consistent with the similar linkers employed in the two arrays. A 5-fold shorter Zn* lifetime (13 ± 2 ps) is found for **Dyad-1**, reflecting more rapid energy

(44) (a) Rodriguez, J.; Kirmaier, C.; Holten, D. *J. Am. Chem. Soc.* **1989**, *111*, 6500−6506.
(45) (a) Gradyushko, A. T.; Sevchenko, A. N.; Solovyov, K. N.; Tsvirko, M. P. *Photochem. Photobiol.* **1970**, *11*, 387−400. (b) Hurley, J. K.; Sinai, N.; Linschitz, H. *Photochem. Photobiol.* **1983**, *38*, 9−14. (c) Kajii, Y.; Obi, K.; Tanaka, I.; Tobita, S. *Chem. Phys. Lett.* **1984**, *111*, 347−349. (d) Kikuchi, K.; Kurabayashi, Y.; Kokubun, H.; Kaizu, Y.; Kobayashi, H. *J. Photochem. Photobiol. A: Chem.* **1988**, *45*, 261−263. (e) Bonnett, R. D.; McGarvey, D. J.; Harriman, A.; Land, E. J.; Truscott, T. G.; Winfield, U. J. *Photochem. Photobiol.* **1988**, *48*, 271−276.
(46) Seybold, P. G.; Gouterman, M. *J. Mol. Spectrosc.* **1969**, *31*, 1−13.
(47) (a) Yang, S. I.; Seth, J.; Strachan, J.-P.; Gentemann, S.; Kim, D.; Holten, D.; Lindsey, J. S.; Bocian, D. F. *J. Porphyrins Phthalocyanines* **1999**, *3*, 117−147. (b) Tomizaki, K.-Y.; Loewe, R. S.; Kirmaier, C.; Schwartz, J. K.; Retsek, J. L.; Bocian, D. F.; Holten, D.; Lindsey, J. S. *J. Org. Chem.* **2002**, *67*, 6519−6534.

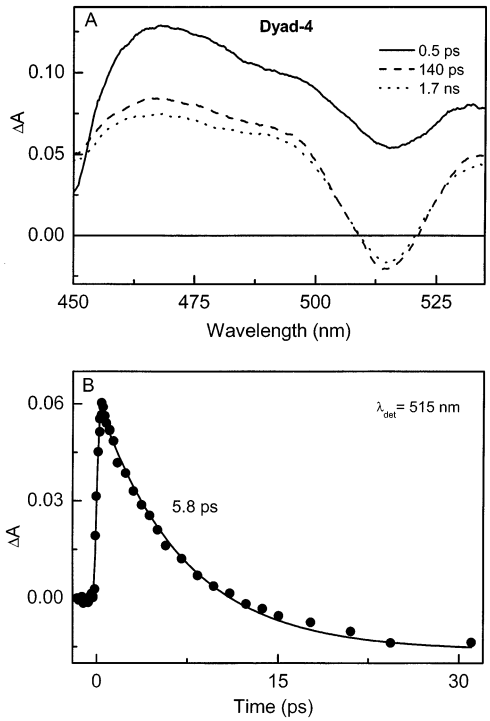

Figure 6. Representative time-resolved absorption spectra (A) and a kinetic profile (B) for **Dyad-4** in toluene at room temperature using predominant excitation of the zinc porphyrin with a 551 nm 130 fs flash. The fit to the kinetic data at 515 nm in (B) gives a time constant of 5.8 ps, and the average value reflecting the Zn* lifetime from measurements at several different detection wavelengths is given in Table 2.

transfer to the free base component than in **Dyad-2** and **Dyad-3** due to the linker being two atoms shorter, along with associated linker electronic characteristics.

Two observations indicate that Zn*Fb → ZnFb* energy transfer is virtually quantitative for **Dyads-1−3** in toluene. First, there is no clear evidence for formation of Zn^+Fb^- in the transient absorption spectra. Second, the Fb* fluorescence yield is comparable using excitation of either subunit, indicating $\Phi_{EnT} > 90\%$. Third, the Zn* lifetime in each dyad is much shorter than that of ∼2 ns for reference porphyrins such as **Zn-16**. Given these findings, the rate constant and quantum yield of Zn*Fb → ZnFb* energy transfer for **Dyads-1−3** in toluene were estimated using the expressions $k_{EnT} = (1/\tau_{dyad}^{Zn*}) - (1/\tau_{ref}^{Zn*})$ and $\Phi_{EnT} = 1 - (\tau_{dyad}^{Zn*}/\tau_{ref}^{Zn*})$. The results are given in columns 7 and 8 of Table 2, with the corresponding yield of electron transfer given in column 9. The results for these dyads in benzonitrile given in Table 2 are based on the fluorescence data, which again indicate a high yield of Zn*Fb → ZnFb* energy transfer and relatively little competing Zn*Fb → Zn^+Fb^- electron transfer taking place.

Dyad-4 in Toluene. Representative transient absorption difference spectra for **Dyad-4** in toluene are shown in Figure 6. Similar to **Dyad-3**, the 0.5 ps spectrum (—) is assigned mainly to Zn*, with a minor contribution of Fb* due to direct excitation. Note the bleaching of the 435-nm zinc porphyrin Soret band on the blue edge of this spectrum. The spectrum at 140 ps (− −) has a deep bleaching in the 515-nm ground-state absorption band of the free base porphyrin and is assigned largely to Fb* formed via energy transfer from Zn*. The relatively minor changes at longer times are again consistent with the long (∼11 ns) Fb* lifetime and high yield of Fb^T. However, the spectra at 140 ps and longer cannot be ascribed solely to Fb* because they clearly still display the edge of 435-nm Soret bleaching of the zinc porphyrin component. This bleaching must reflect a contribution from Zn^+Fb^- formed by electron transfer from Zn* to the free base porphyrin (Figure 1A). In contrast, no such bleaching is seen in the longer-time spectra for **Dyad-3** in toluene (Figure 5A), supporting the very high energy-transfer yield discussed above.

On the basis of the Soret bleach at ∼460 nm at 140 ps versus 0.5 ps, the fraction of Zn* that decays by Zn*Fb → Zn^+Fb^- electron transfer is estimated to be 0.35 for **Dyad-4** in toluene, with the remainder (0.65) assigned to Zn*Fb → ZnFb* energy transfer. The average Zn* lifetime of 5.4 ± 0.7 ps for **Dyad-4** in toluene was determined from measurements at a number of probe wavelengths (e.g., Figure 6B). From these values, the rate constants for Zn* energy and electron transfer for **Dyad-4** in toluene are approximated by $k_{EnT} = (5.4\text{ ps})^{-1}\cdot 0.65 = (8.3\text{ ps})^{-1}$ and $k_{ET} = (5.4\text{ ps})^{-1}\cdot 0.35 = (15.4\text{ ps})^{-1}$ (Table 2).

Dyad-4 in Benzonitrile. The competition between energy and electron transfer from Zn* was further probed for **Dyad-4** in benzonitrile. It can be expected that this polar solvent will make electron transfer more facile owing mainly to the lower energy of the charge-separated state. As for **Dyad-4** in toluene, the spectra for this array in benzonitrile after Zn* decay show features characteristic of Fb* as well as features involving the zinc porphyrin that we assign to state Zn^+Fb^-. Again, on the basis of the magnitudes of these spectral features, the yield of Zn*Fb → Zn^+Fb^- electron transfer is estimated to be ∼50%, with a comparable yield for Zn*Fb → ZnFb* energy transfer (Table 2). This increase in the electron-transfer yield from ∼35% in toluene must derive primarily from an associated increased rate constant of this process, consistent with the observed shortening of the Zn* lifetime from ∼5.5 ps in toluene to ∼3.0 ps in benzonitrile. The rate constants for Zn* energy and electron transfer for **Dyad-4** in benzonitrile are thus both determined to be $(3.0\text{ ps})^{-1}\cdot 0.50 = (6.0\text{ ps})^{-1}$.

Dyad-5 in Toluene. The time evolution of the absorption difference spectra of **Dyad-5** in toluene (see Supporting Information) shows that the excited state of the aryl-substituted zinc porphyrin decays with a time constant of 2.5 ± 0.2 ps, which is much shorter than the reference value of ∼2 ns. During this time, there is concomitant formation of bleaching in the ground-state absorption bands of the imine-substituted zinc porphyrin. These data are consistent with a high yield of $Zn_a{*}Zn_i \rightarrow Zn_aZn_i{*}$ energy transfer (Figure 1B), but due to spectral overlap, it is difficult to assess the extent of competing charge transfer from these data alone. The static fluorescence data give an energy-transfer yield of ≥80% resulting in an electron-transfer yield of ≤20% (Table 2). Combining with the Zn* lifetime gives an energy-transfer rate constant of $k_{EnT} \sim (2.5-3.1\text{ ps})^{-1}$.

General Comparisons. In **Dyads-1−3**, the linker contains a phenyl ring attached to each porphyrin with the imine unit

between the phenyl rings. All three dyads afford nearly quantitative Zn*Fb → ZnFb* energy transfer in toluene and >90% in benzonitrile. Subsequent ZnFb* → Zn^+Fb^- hole-transfer yields are <10% in toluene and <25% even in the polar solvent benzonitrile. Together, these findings augur well for efficient energy transfer and subsequent utilization of the energy available at the output unit in these three self-assembled entities when incorporated in larger architectures.

The salicylaldimine- and acyl-hydrazone-based linkers used in **Dyad-2** and **Dyad-3**, respectively, afford similar Zn*Fb → ZnFb* energy-transfer rates of $\sim(70\ ps)^{-1}$ in toluene. **Dyad-3** differs from **Dyad-2** primarily in the presence of a hydrogen-bonding interaction that should afford higher stability of the assembly. **Dyad-1** exhibits a 5-fold greater energy-transfer rate of $(13\ ps)^{-1}$ and a slightly higher yield (99%). The more rapid energy transfer is consistent with the imine-based linker in **Dyad-1** being two-atoms shorter than those employed in **Dyad-2** and **Dyad-3** (although differences in electronic characteristics may also play a role).

In **Dyad-4**, the imine portion of the acylhydrazone unit is directly attached to the zinc porphyrin. Thus, **Dyad-4** also has a shorter linker than **Dyad-2** and **Dyad-3**. This shorter linker, perhaps in conjunction with electronic effects from direct attachment to the macrocycle, again affords a significantly increased energy-transfer rate for **Dyad-4** in toluene of $(8.3\ ps)^{-1}$ compared to $\sim(70\ ps)^{-1}$ for **Dyad-2** and **Dyad-3**. However, **Dyad-4** suffers from a similar increase in the yield of competing Zn*Fb → Zn^+Fb^- electron transfer even in the nonpolar medium toluene (~35% for **Dyad-4** compared to ≤8% for **Dyads-1**−**3**). The subsequent quenching of Fb* via hole transfer to the zinc porphyrin is also larger in **Dyad-4** than in **Dyads-1**−**3**. Thus, the increased Zn*Fb → ZnFb* energy-transfer rate in **Dyad-4** comes at the expense of an increased yield of two wasteful charge-transfer processes. On the other hand, a useful aspect of the porphyrin-imine direct attachment motif is that it allows the generation of a module containing two electronically distinct zinc porphyrins. The resulting **Dyad-5** has the fastest energy transfer of all the dyads $[\sim(3\ ps)^{-1}]$, a Zn_a*Zn_i → Zn_aZn_i* energy-transfer yield of ≥80% in toluene, and significantly suppressed subsequent hole transfer (~10% even in benzonitrile) compared to ZnFb **Dyad-4**. Thus, **Dyad-5** has favorable characteristics that may be exploited in more elaborate molecular architectures.

In summary, for the ZnFb dyads, the linker motif employed in **Dyad-1** is far superior to that in **Dyad-4** when the goal is efficient energy transfer on the ~10 ps time scale. We note also that the energy-transfer rate in the self-assembled **Dyad-1** $[(13\ ps)^{-1}]$ is actually larger than that found for covalently linked dyads employing diphenylethyne $[(24\ ps)^{-1}]$ or diphenylbutadiyne $[(37\ ps)^{-1}]$ linkers, and only modestly smaller than for a *p*-phenylene linker [(~3.5 ps)].[43] Although the energy-transfer rate is smaller in **Dyad-2** and **Dyad-3** $[\sim(70\ ps)^{-1}]$, near quantitative energy transfer is maintained.

Conclusions

We have shown here that porphyrins can be joined using an imine-based attachment motif that affords rapid and efficient excited-state energy transfer while maintaining weak linker-mediated inter-porphyrin electronic interactions. The relatively weak interactions allow key intrinsic properties (redox, photophysical) designed into the isolated components to be largely retained in the arrays. Accordingly, the desired characteristics of diverse architectures of increasing complexity can be reasonably anticipated from those of simple dyad and triad motifs. Collectively, the studies described herein indicate that the self-assembly approach can be implemented to afford porphyrin-dyad modules that have comparable or even enhanced energy-transfer characteristics relative to those of more conventional covalently linked systems. Additional variations on the theme of self-assembly are examined in the following paper, where arrays composed of two porphyrins linked via an intervening bis(dipyrrinato)-metal linker are described.

Acknowledgment. This research was supported by the NSF (Grant CHE-9988142). Mass spectra were obtained at the Mass Spectrometry Laboratory for Biotechnology at North Carolina State University. Partial funding for the Mass Spectrometry Laboratory for Biotechnology at North Carolina State University was obtained from the North Carolina Biotechnology Center and the NSF.

Supporting Information Available: Absorption/emission spectra of all the dyads and reference compounds in toluene and benzonitrile; time-resolved absorption spectra and kinetic profiles for **Dyad-1**, **Dyad-2**, and **Dyad-5** in toluene and **Dyad-4** in benzonitrile. Complete Experimental Section including the synthesis of 4-(2,4-dioxopentan-3-yl)benzaldehyde and spectral data (absorption, fluorescence, ^{1}H NMR, VT-NMR, LD-MS) for all new compounds. This material is available free of charge via the Internet at http://pubs.acs.org.

IC034558U